

C. Sozzi, A. Bruschi, D. Farina, L. Figini, M. Lennholm, A. Moro
and JET EFDA contributors

Feasibility of an ECRH System for JET: Options for an ECRH/ECCD Launcher Design

“This document is intended for publication in the open literature. It is made available on the understanding that it may not be further circulated and extracts or references may not be published prior to publication of the original when applicable, or without the consent of the Publications Officer, EFDA, Culham Science Centre, Abingdon, Oxon, OX14 3DB, UK.”

“Enquiries about Copyright and reproduction should be addressed to the Publications Officer, EFDA, Culham Science Centre, Abingdon, Oxon, OX14 3DB, UK.”

The contents of this preprint and all other JET EFDA Preprints and Conference Papers are available to view online free at www.iop.org/Jet. This site has full search facilities and e-mail alert options. The diagrams contained within the PDFs on this site are hyperlinked from the year 1996 onwards.

Feasibility of an ECRH System for JET: Options for an ECRH/ECCD Launcher Design

C. Sozzi¹, A. Bruschi¹, D. Farina¹, L. Figini¹, M. Lennholm^{2,3}, A. Moro¹
and JET EFDA contributors*

JET-EFDA, Culham Science Centre, OX14 3DB, Abingdon, UK

¹*IFP-CNR, EURATOM-ENEA-CNR Association, Milan, Italy*

²*EFDA, Close Support Unit, Culham Science Centre, OX14 3DB, Abingdon, OXON, UK*

⁴*Oak Ridge National Laboratory, Oak Ridge, TN 37831, USA*

⁵*A3European Commission, B-1049 Brussels, Belgium*

* *See annex of F. Romanelli et al, "Overview of JET Results",
(Proc. 22nd IAEA Fusion Energy Conference, Geneva, Switzerland (2008)).*

Preprint of Paper to be submitted for publication in Proceedings of the
16th Joint Workshop on Electron Cyclotron Emission and Electron Cyclotron Resonance Heating,
Sanya, China.

(12th April 2010 - 15th April 2010)

ABSTRACT.

A study has been conducted to evaluate the feasibility of installing an ECRH plant on the JET tokamak. The possible options for the wave launching system for JET have been investigated, assuming a frequency of 170 GHz, the use of an evacuated transmission line and the availability of an entire JET mid-plane port for the launching system. Applications include NTM and sawteeth control, core heating and current drive, current profile tailoring .

1. GUIDELINES FOR THE PRELIMINARY DESIGN

While in principle ECRH/ECCD systems in toroidal fusion devices are nowadays nearly “standard” equipment, serious issues for the launcher design come when high performance, extended flexibility and lack of space are among the constraints of the project. This is the case of JET where the most powerful ECRH plant worldwide in an existing machine, with wide poloidal and toroidal steering, real time capabilities, and tritium-grade vacuum integration is being considered for installation. The technical requirements for the launcher have been specified after an extensive wave propagation study related with the range of the ITER-oriented physics applications desirable for JET [1]. The main requirements to be fulfilled are:

- Power capability of 10 MW delivered into plasma
- 20sec pulse duration repeated every 15 minutes
- Steering range of $\Delta\beta = \pm 30^\circ$ (toroidal, shot to shot positioning), $\pm 25^\circ < \Delta\alpha < \pm 5^\circ$ (poloidal, real time controlled)
- Optical performances (power and driven current density) good enough for NTM control (JCD current channel 5–10cm wide ($\Delta\rho < 0.1$) [2,3] in an extended absorption range (1–1.5 m long, depending on the plasma magnetic field and island location)
- Inclusion of the ITER poloidal steering mechanism [4,5] with minimum modifications in terms of design and functionalities
- Port integration compatible with plug-in installation (no or minimum use of remote handling and/or fixed in-vessel installations)

For what concerns the antenna, three design options (Figure 1) have survived the initial stage of the feasibility study. All the options use two nearly identical modules, vertically displaced, each one occupying half of the available volume, including the ITER steering mechanism (see Table 1) and using 2×6 corrugated waveguides of 63.5 mm inner diameter as input. Each beamline is equipped with a focusing mirror positioned in front of the waveguide redirecting the beam towards the steering unit. The other mirrors in the system are flat. The toroidal mechanism is not yet identified in detail and is only considered in term of required functionalities (i.e. angular range and needed clearance).

Option L1: the whole steering system is placed in the narrow part of the JET port close to the plasma boundary. A modified ITER-like mechanism mounts the poloidal mirror tangentially. The toroidal steering is realized rotating the whole poloidal mechanism or the mirror only around a nearly vertical axis.

Option L2: an unmodified ITER-like mechanism in the rear part of the JET port provides the poloidal steering. The toroidal steering is obtained moving the whole mechanism in such a way that the beams can enter the plasma either directly or through 1 or 2 bounces on two large, fixed, flat (non parallel) side mirrors. This layout provides a range of toroidal injection angles with forbidden angular windows.

Option L4: an unmodified ITER-like mechanism in the rear part of the JET port provides the poloidal steering. The toroidal injection is obtained steering one of the side mirrors with 1 or 2 bounces towards the plasma. This layout provides a nearly continuous range of toroidal angles. significant advantages in terms of achievable steering range and appears suitable for easier port integration. The remainder of the paper is therefore mainly focused on option L4.

2. STEERING RANGE

The steering range is expressed in terms of the poloidal angle α (between the horizontal plane at constant z and the poloidal component of the beam) and the toroidal angle β (the angle between the beam and the poloidal plane).

The achievable steering range for option L4 in the α, β plane is shown in Figure 2 (shaded area). It spans about $\pm 30^\circ$ toroidally and $\pm 30^\circ$ poloidally. In order to cover most of the plasma volume, the upper and lower ranges are generally separate, except for a superposition region around the equatorial plane represented by the darker area. A small forbidden gap of about $\pm 0.5^\circ$ due to the 1 to 2 bounces range transition is located around 1° toroidal injection angle.

3. FOCUSING OPTICS AND BEAM SIZE OPTIMIZATION

The focusing mirror parameters have been optimized with the criterion of minimizing the beam size in a reference absorption position in the plasma, corresponding to $R = 2.5\text{m}$ with radial injection. The input parameters for the optimization are the input beam waist ($w_{0\text{in}} = 20.4\text{mm}$ at the waveguide's tip) and the input distance from the waveguide to the focusing mirror $d_{0\text{in}}$. The output parameters (for each value of $d_{0\text{in}}$) are the focal length f of the mirror and the ellipsoidal surface equation obtained matching the phase front curvature on the mirror surface.

Figure 3 shows the output beam waist $w_{0\text{out}}$ and the beam dimension w_{pl} at $R = 2.5\text{m}$ versus $d_{0\text{in}}$. As expected, larger input distance $d_{0\text{in}}$ gives better focusing in the plasma, with little effect on $w_{0\text{out}}$. Figure 4 compares the beam size versus the propagation distance from the input waveguide for the different layouts. For L4 option $d_{0\text{in}} = 800\text{mm}$, $f = 1037\text{mm}$ and mirror diameter $D = 100\text{mm}$ ($\cong 3w$ at $d_{0\text{in}}$) have been considered, as longer input distances seem to be impractical. Dots in the figure are physics optics computation [6] including beam truncation effects.

The resulting beam size is in line with the requirements, but safer margins can be obtained with a mode converter artificially increasing the effective $d_{0\text{in}}$. Such device is currently being designed.

4. POWER DISTRIBUTION ON MIRRORS

Physics optics computation have been performed to compute the power density and beams

distribution on the mirrors. Figure 5 shows the beams footprint on the poloidal steering mirror for the L4 options, with the optical parameters specified above. The increased contrast area on one of the beams marks the $1/e^2 = -8.7\text{dB}$ contour including 86.46% of the equivalent gaussian beam power. The peak power density is $97\text{kW}/\text{cm}^2$ assuming 1MW beam power. The average power density in the beam radius (white contour) is $55\text{kW}/\text{cm}^2$. These values are rather high but seems acceptable for a transient system [7].

5. OPTIMISATION OF THE BEAMS SUPERPOSITION IN THE PLASMA

Applications such the NTM control and suppression are critically dependent from the driven current density in the magnetic island location and therefore the superposition of the beams along an extended region is a key factor in a multi-beam system operating over a range of magnetic fields. Assuming the spacing among the input waveguides of 10cm and the L4 layout the maximum achievable current density has been computed for the resonance on the $q = 3/2$ magnetic surface at $B = 2.8\text{T}$ using the beam tracing code GRAY [8]. An optimal geometrical convergence of the beams corresponding to $\delta\alpha = 2^\circ$ has been derived. Then the driven current profile has been evaluated for magnetic fields $2.6 < B < 3.2\text{ T}$. In this range the current channel broadening (FWHM) is below 20% of the optimized case, being smaller at the lower extreme of the magnetic field range. This broadening corresponds to a reduction of about 12% of the peak current density.

The convergence of $\delta\alpha$ between beams launched from different z position of the same module is achievable by introducing a similar tilt in the orientation of the focusing mirrors.

CONCLUSIONS

A few layout options for the ECRH/ECCD launcher of JET have been studied. From the feasibility point of view, at least one of them (L4) is compliant with the requirements and does not present major technical drawbacks.

ACKNOWLEDGMENTS

This work, carried out under the European Fusion Development Agreement, supported by the European Communities and “Istituto di Fisica del Plasma P.Caldirola – CNR”, has been carried out within the Contract of Association between EURATOM and IFP. The views and opinions expressed herein do not necessarily reflect those of the European Commission or IFP. Authors are indebted to the colleagues of the EC/ECRH community at ITER/IO, F4E, CRPP Lausanne, IPP Greifswald

REFERENCES

- [1]. G. Giruzzi et al., this conference
- [2]. S. Nowak, this conference
- [3]. D. Farina, L. Figini, this conference
- [4]. R. Chavan et al., Fusion Engineering and Design **74**, 437–441, (2005)
- [5]. A. Collazos et al., Fusion Engineering and Design **84**, 618–622, (2009)

- [6]. K. Pontoppidan, GRASP® Tech. Description, TICRA, Denmark (2005).
- [7]. F. Sanchez et al., Fusion Engineering and Design **84**, 1702–1707, (2009)
- [8]. D. Farina, Fusion Sci. Technol. **52** 154 (2007)

Poloidal steering mechanism

Size	~250 (L) × 245 (D) mm, cylindrical shaped
Actuator	Pneumatic (He gas), servo-valve 3.5 – 21.5 bar
Range	+/- 7° (rotation around symmetry axis)
Speed	Full range < 3 secs
Accuracy	0.05°

Table 1. Main characteristics of the ITER steering mechanism

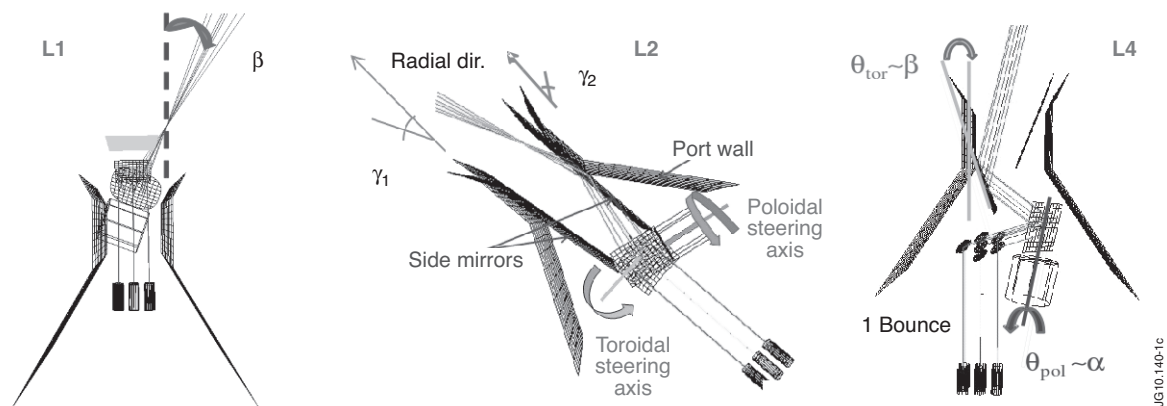


Figure 1: Options for the steering unit layout (top view, not in scale). β is the toroidal injection angle, γ_1 and γ_2 are the fixed angular positions of the side mirrors (with respect to the radial direction), θ_{tor} (θ_{pol}) is the adjustable angle of the toroidal (poloidal) steering mechanism.

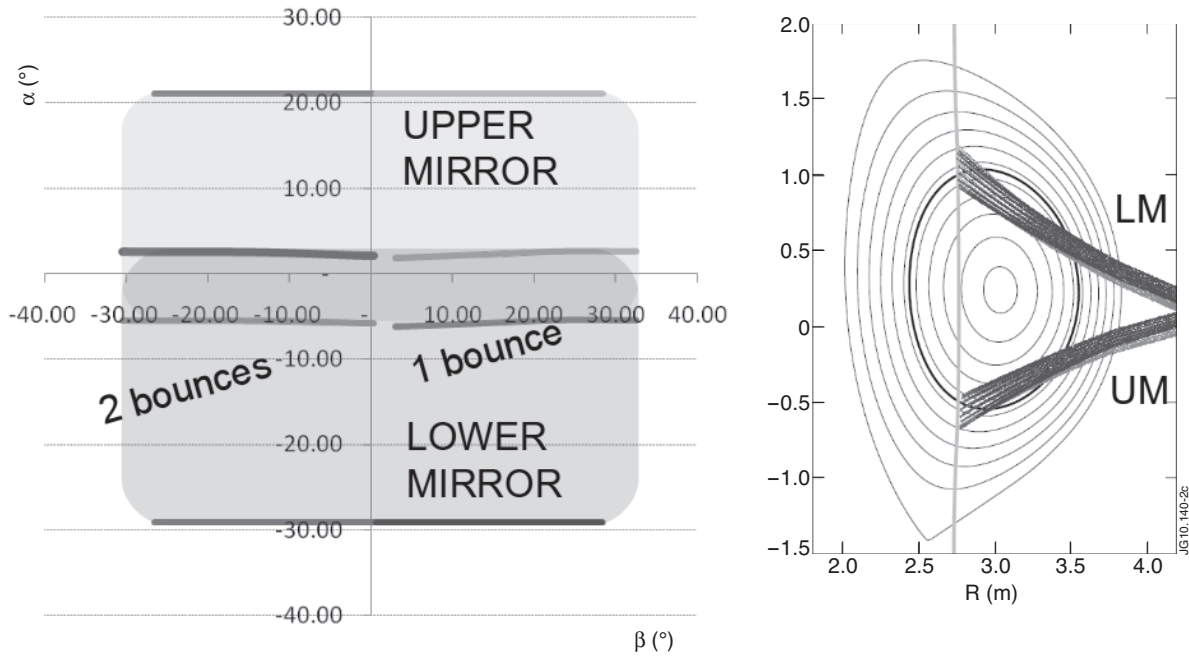


Figure 2: On left: steering range obtained with the L4 layout design. Note that positive α 's are downward. On right: beams paths for the upper and lower steering units ($B=2.8T$, resonance near the $q=3/2$ magnetic surface). Beams paths from UM and LM crosses outside the last closed magnetic surface.

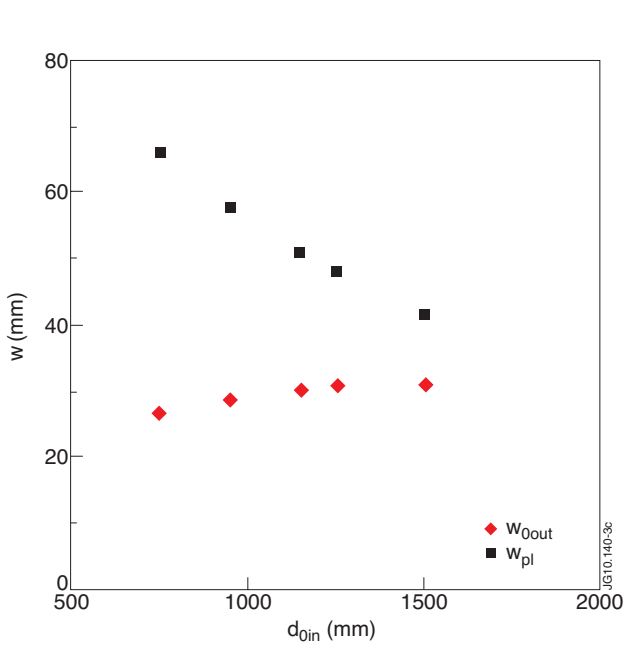


Figure 3: Beam waist (w_{0out}) and size (w_{pl}) at the reference absorption location as a function of the distance from the input waveguide to the focusing mirror.

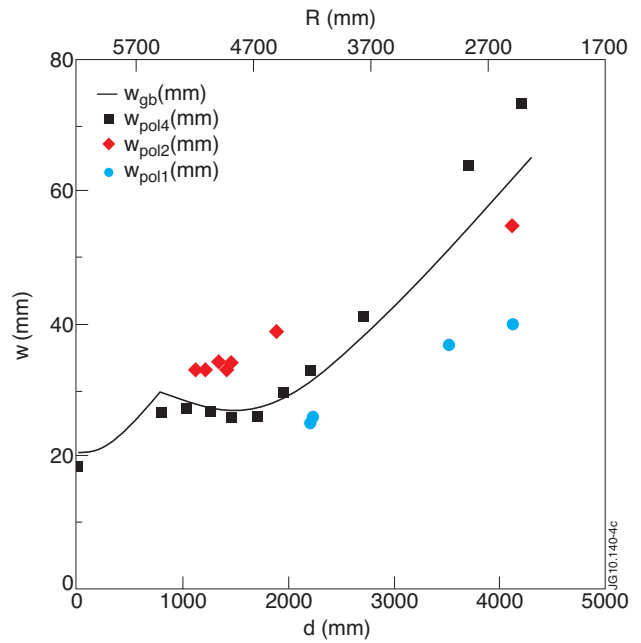
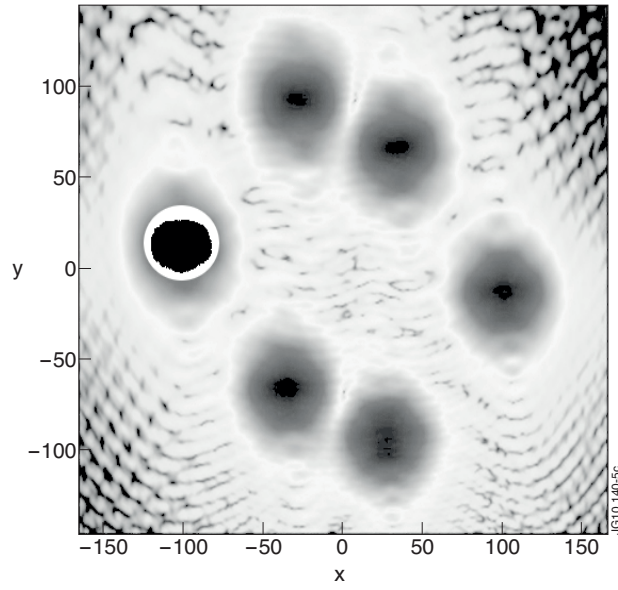


Figure 4: Beam size along the propagation distance d (and plasma radius R) from the waveguide exit computed with a physics optics tool (dots) for the various layout's options. Line represents the corresponding gaussian beam propagation for L4 option.



*Figure 5: Power distribution on the poloidal steering mirror (see text).
Fringe pattern in the corners are artifacts. Units on axis are mm.*